Modelling of Electromagnetic Fields for Shielding Purposes Applied in Instrumentation Systems

Ahmad M. Dagamseh [1*], Qasem M. Al-Zoubi [1], Qasem M. Qananwah [2], and Hamzeh M. Jaradat [3]

[1] Department of Electronics Engineering, Hijjawi Faculty for Engineering Technology
Yarmouk University, Irbid, P.O. Box 21163, Jordan
*a.m.k.dagamseh@yu.edu.jo, qzabi50@yu.edu.jo

[2] Department of Biomedical Systems and Informatics Engineering, Hijjawi Faculty for Engineering Technology
Yarmouk University, Irbid, P.O. Box 21163, Jordan
qasem.qananwah@yu.edu.jo

[3] Department of Telecommunications Engineering, Hijjawi Faculty for Engineering Technology
Yarmouk University, Irbid, P.O. Box 21163, Jordan
hamzehjaradat@yu.edu.jo

Abstract ─ In any sensory system, the Electromagnetic (EM) shielding of the channel-carrying signal is a fundamental technique to provide a noise-immune measurement system. Severe failures and uncertainty may occur if the external EM fields interfered with the measurements. Typically, the shielding is realized by enclosing the channel-carrying signal with thin-conductive hollow structures. However, with such structures, it is required to provide access to the interior components from the outside, for wires' connections, or better heat dissipation. This can be considered as a weakness in such the external magnetic fields can penetrate through the shielding structure. In this paper, the EM shielding effectiveness is considered for long hollow-cylinder structures with slots. The induced eddy current in thin-conductive shielding systems with slots together with the magnetic fields at different conditions are modeled. The objective is to determine the impact of the integrated slots along with the structure. The influence of the slots' sizes ($\boldsymbol{\alpha}$) and position relative to the excitation magnetic field (i.e., the declination angle ($\boldsymbol{\beta}$)) are investigated to evaluate the shielding effectiveness by means of the determination of the shielding factor. The results reveal the inherent relationship between the shield parameters and shielding effectiveness. The shielding effectiveness deteriorates by the slots' integration within the shielding surface. However, decreasing the size of the slots improves the shielding, significantly, towards the shielding effectiveness of the continuous cylindrical structure. Additionally, utilizing the symmetry in the structure positioning the slots in the direction perpendicular to the magnetic field flux improves the shielding effectiveness, drastically. Such a model can be considered to evaluate the degree of effectiveness or success of integrating opening slots within the shielding structure, which can be applied to different types of instrumentation systems specifically at the sensor-electronics interface.

Index Terms ─ Hollow cylinder, instrumentation system shielding, magnetic field, shielding effectiveness.

I. INTRODUCTION

Recently, electronic devices and technologies have been developing rapidly. The notable progress and systems' integrity, specifically in devices' structure, PCB designs, and packaging, led to an increase the complexity. The system requirements to overcome the error, reduce Electromagnetic Interference (EMI), and generate or transmit free-of-noise signals with proper timing have been considered intensively. Specifically, the EMI, as the major source of measurement errors in various disciplines, has been treated to make the electronic system immune. One of these disciplines is sensor design and instrumentation, where Electromagnetic Shielding (EMS) is frequently used to block or reduce either the emitted or intruded noise components. Metal sheets (e.g. aluminum, copper, etc…) formed in different structure designs can be used to fit the electronics enclosures [1,2].

EMS can be considered to design reliable systems, especially in critical applications. Examples of such systems include industry, military, medical, electric vehicle, sensors, and aerospace electronic devices, where the results of failure can extend from data loss to death [3]. However, there are no comprehensive structure designs to perform shielding. Therefore, in instrumentation

Submitted On: January 7, 2021
Accepted On: July 8, 2021

https://doi.org/10.47037/2021.ACES.J.360817

systems with EMS, the shield encloses the signal path in the entire instrumentation channel. Particularly, at the interfacing side between the sensor and the electronics, the role of EMS can be significant as the sensor's signal is still weak at this interface.

The integration of EMS in sensors has been studied intensively in the literature. There will be great advantages in combining the sensation techniques and EMS to perform proper measurements and improve the robustness and accuracy of the instrumentation system. Rienzo in his paper modeled the magnetic sensors to measure high AC and DC currents based on magnetic field sensing [4]. The application of EMS in instrumentation was used to reduce the measurement error using a ferromagnetic or conductive material. Shielding can be utilized to improve the measurements and the detection limit of the capacitive sensors. This can be attained by reducing the effects of both external noise and parasitic capacitances. With such a scheme, Dagamseh et al. modified the design of the capacitive-based artificial hair sensor using wafer-level and printed-circuit-board shielding [5]. The modified design improved the resolution of the measurement (i.e., performing localized measurement) and allowed measuring the capacitance changes originated from a single-hair sensor. Consequently, the detection limit of the new sensor design is improved down to 1 mm s–1 airflow amplitude with significant improvement in the directivity. Yang et al. presented a current sensor based on a giant magnetoresistance system with magnetic shielding [6,7]. The sensitivity and linearity of the sensors were considered by reducing the error due to the magnetic field. The results show that the sensor has a low nonlinearity error of less than 0.8% for the range of 10 mA to 20A for frequencies up to 200 kHz.

Screening by thin conductors with simple geometrical forms like planes, hollow cylinders, and hollow spheres has been investigated in the literature. Kaden investigated the screening effect of thin layers with angles and seats [8]. Lopez et al. provided a comparison between two conductive textiles with a wire mesh screen or with compact material to assess the shielding effectiveness [9]. The results showed good agreement between the modeling and measurement results with a 3 dB deviation at 1 GHz for the wire mesh model compared with a 2 dB deviation at 1.5 GHz for the compact material.

Another fundamental issue related to shielding is the shape of the shield. Azizi et al. have considered modeling the shielding effectiveness of aperture in a rectangular enclosure using circuit modeling and finite-difference time-domain method [10]. The results showed that the square and circular apertures are better to use than the rectangular shapes in electromagnetic shielding. Park et al. considered the integration of periodic metal strips within a conventional ferrite plate [11]. The period of the metal strip and the source position concerning the metal strips were considered. However, the analysis was provided for very thin strips. Fagnard et al. modeled the effect of introducing slits within a cylinder shield structure [12]. With his work, the analysis considered the magnetic properties of a hollow cylinder specifically with two axial slits that cut the cylinder in equal halves.

Several studies have analyzed and modeled the eddy currents in magnetic conductors and investigated the shielding effectiveness for different shielding structures [13-21]. H. El-Maghrabi investigated the shielding effectiveness and determined the electromagnetic shielding effectiveness of two cascaded wire-mesh sheets. The model results were compared with experiments and good agreement was obtained [13]. R. Araneo studied the effect of the shield parameters and position of the source on the effectiveness of the shield at low-frequency near0field magnetic sources [14]. Mayergoyz et al. analyzed the eddy currents for elliptical polarization of the magnetic field [17]. Delinger modeled the magnetic field inside a long cylindrical hole in a long cylindrical conductor [18]. The solution involved the summation of the magnetic fields of the current centered at the conductor and the opposite direction centered at the hole. Babic et al. modeled the magnetic field of a hollow cylinder with finite thickness in three dimensions with a longitudinal current component [19]. Sailing et al. have utilized the magnetic field of the direct current to identify the cracks in conductors [20]. A model to identify surface cracks with an elliptic shape was provided. Kvitkovic et al. investigated the shielding effectiveness within the inhomogeneous magnetic field [21].

For various instrumentation systems, the shielding at the sensor-electronics interface is a critical node; as the signal is weak. Electromagnetic shielding can be performed to protect the measured signal and thereby the accuracy of the measurement system. In this paper, the magnetic field has been modeled using a cylindrical geometrical structure with slots, taking into consideration the induced eddy currents. The target is to evaluate the impact of integrating slots within the shield in terms of shielding effectiveness utilizing studying the characteristics of the shield. These slots can be, thereby, controlled for the optimal performance of the entire instrumentation system to provide an access to the sensor side or to the interfacing electronics.

II. SYSTEM MODELING

The magnetic shielding depends on the material properties, the shield geometry, and the amplitude of the magnetic field. In this work, we investigate the effect of shielding structures on the field shape and the characteristics of the shield. A Long-hollow cylinder structure with integrated lateral slots for different designs is considered. The models will be based on determining the shape of the eddy currents in the

shielding structure and the magnetic flux through the slot to investigate the magnetic flux penetration. It is assumed that the skin-depth (δ) is much more than the thickness of the conductive layer with $\delta = \frac{1}{\sqrt{\pi\mu f\sigma}}$ with μ, f and σ are the magnetic permeability ($\frac{N}{A^2}$), frequency (Hz), and conductivity ($\frac{S}{m}$), respectively [22].

The solution for the eddy currents with two axial slots, taking into consideration the symmetry of the structure, consists of the following procedure and assumptions:

- The general solution for the homogeneous problem to determine the vector potential A (inside and outside the shielding surface) can be obtained using the solution of the Laplace equation. The excited magnetic alternative field B can then be obtained using this solution.
- The coefficients of the solution can be defined using the boundary conditions. At the boundaries of both regions (i.e., above and below the shielding structure) the following conditions can be applied:

$$A_1 = A_{2.}, \tag{1}$$

and

$$(H_{t1} - H_{t2}) = K, \tag{2}$$

where H_{t1} and H_{t2} are the magnetic field intensity outside and inside the shielding surface, respectively.

- The surface current density K can be determined using the law of induction along the circumference of the cylinder with thickness d according to:

$$K = \begin{cases} -j\omega x d A_{1,} \\ \text{for: } -\pi + \beta + \frac{\alpha}{2} \le \varphi \le \beta - \frac{\alpha}{2} \\ \text{and } \beta + \frac{\alpha}{2} \le \varphi \le \pi + \beta - \frac{\alpha}{2} \\ 0, \quad \text{else} \end{cases}. \tag{3}$$

- According to equ. (3), the surface current can be expanded in terms of the solutions for the coefficients of vector potentials A_1 and A_2 and substitute it in equ. (2). This results in a linear system of equations that can be used to find the coefficients of the Laplace solution.
- The vector potential is considered as the sum of the exciting vector potential A_o (outside the shielding surface) and the vector potential of the generated eddy current A_i (inside the shielding surface) with:

$$A = A_i + A_o. \tag{4}$$

A long hollow-cylinder with lateral slots the homogeneous alternating field H_o is considered. The magnetic field is oriented perpendicularly to the cylinder. To simplify the solution through the distribution of currents, the thickness of the cylinder wall (d) is assumed to be small. The width of the slot is defined by the angle (α). The position of the slot, in reference to the direction of the field H_o, is described by the angle (β). Figure 1 shows the design parameters of the hollow-cylinder shielding structure.

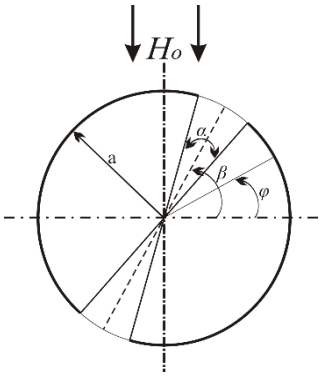

Fig. 1. A schematic representation for the hollow-cylinder shielding structure with lateral slots and the definitions of the angles (α, β, and φ).

The solution of the Laplace equation for the vector potential A in polar coordinates can be represented as shown in equ. (5):

$$\left.\begin{aligned} A_o(\rho,\varphi) &= \mu a H_0 \left[\frac{\rho}{a}\cos\varphi + \sum_{n=1}^{\infty}\left(\frac{a}{\rho}\right)^n (C_n \cos n\varphi + D_n \sin n\varphi)\right] \\ &\text{for } \rho \ge a \\ A_i(\rho,\varphi) &= \mu a H_0 \left[\frac{\rho}{a}\cos\varphi + \sum_{n=1}^{\infty}\left(\frac{\rho}{a}\right)^n (C_n \cos n\varphi + D_n \sin n\varphi)\right] \\ &\text{for } \rho \le a \end{aligned}\right\}, \tag{5}$$

where a is the cylinder radius, C_n and D_n are the solution coefficients.

Due to the symmetry in the design of the system, the vector potential analysis can be performed with the odd numbers n (as $A(\rho,\varphi) = -A(\rho,\varphi+\pi)$. To simplify the solution this property is used at the end of the analysis. The boundary condition in equ. (1) is satisfied by this form of solution and the surface current density becomes at $\rho = a$:

$$K(\varphi) = 2H_0 \sum_{n=1}^{\infty} n(C_n \cos n\varphi + D_n \sin n\varphi). \tag{6}$$

Because of the slots, the structure is not symmetrical along a single axis. Accordingly, equ. (3) can be represented as shown in equ. (7):

$$\left.\begin{aligned} K &= -j\omega\mu x da H_0 \times \left[\cos\varphi + \sum_{n=1}^{\infty}(C_n \cos n\varphi + D_n \sin n\varphi)\right], \\ &\qquad \text{for: } -\pi+\beta+\frac{\alpha}{2} \le \varphi \le \beta-\frac{\alpha}{2} \quad \text{and} \quad \beta+\frac{\alpha}{2} \le \varphi \le \pi+\beta-\frac{\alpha}{2} \\ K &= 0, \qquad \text{for: } \beta-\frac{\alpha}{2} < \varphi < \beta+\frac{\alpha}{2} \quad \text{and} \quad \pi+\beta-\frac{\alpha}{2} < \varphi < \pi+\beta+\frac{\alpha}{2} \end{aligned}\right\}, \tag{7}$$

with constants coefficients C_n and D_n that should be determined.

Utilizing these boundary conditions at the surface in equ. (7), the surface current density can be expanded in Fourier series form as shown in equ. (8):

$$K(\varphi) = \sum_{m=1}^{\infty}(A_m \cos m\varphi + B_m \sin m\varphi). \tag{8}$$

where:

$$\left.\begin{aligned} A_m &= c_m(\pi-\alpha) - \sum_{n=1}^{\infty}(c_n t_{mn} + d_n q_{mn}) - \sum_{\substack{n=1 \\ n\neq m}}^{\infty}(c_n s_{mn} + d_n p_{mn}) \\ B_m &= d_m(\pi-\alpha) - \sum_{n=1}^{\infty}(c_n q_{mn} - d_n t_{mn}) + \sum_{\substack{n=1 \\ n\neq m}}^{\infty}(c_n p_{mn} - d_n s_{mn}) \end{aligned}\right\}, \tag{9}$$

in such

$$\left.\begin{aligned} d_n &= -j\omega\mu x da H_0 . D_n \\ c_n &= -j\omega\mu x da H_0 . C_n \end{aligned}\right\}, \quad \text{for } n \neq 1. \tag{10a}$$

$$c_1 = -j\omega\mu x da H_0(1+C_1), \quad \text{for } n = 1. \tag{10b}$$

and:

$$\left.\begin{aligned} p_{mn} &= \frac{1}{n-m}.\sin[(n-m)\beta].\sin[(n-m)\frac{\alpha}{2}] \\ q_{mn} &= \frac{1}{n+m}.\sin[(n+m)\beta].\sin[(n+m)\frac{\alpha}{2}] \\ s_{mn} &= \frac{1}{n-m}.\cos[(n-m)\beta].\sin[(n-m)\frac{\alpha}{2}] \\ t_{mn} &= \frac{1}{n+m}.\cos[(n+m)\beta].\sin[(n+m)\frac{\alpha}{2}] \end{aligned}\right\}. \tag{10c}$$

The left sides of equ. (6) and equ. (8) are identical to the right sides. This results in two linear-system of equations to determine the constants C_n and D_n for the expression of the vector- potentials, represented in equ. (5). The coefficient matrix that defines C_n and D_n can be represented as:

$$\begin{bmatrix} e & f \\ u & v \end{bmatrix}\begin{bmatrix} C \\ D \end{bmatrix} = \begin{bmatrix} g \\ w \end{bmatrix}. \tag{11}$$

Accordingly, the elements of the coefficient matrix are defined as follows:

$$\left.\begin{aligned} e_{mn} &= s_{mn} + t_{mn} \quad , \quad f_{mn} = p_{mn} + q_{mn} \\ u_{mn} &= q_{mn} - p_{mn} \quad , \quad v_{mn} = s_{mn} - t_{mn} \end{aligned}\right\} \text{ for } m \neq n, \tag{12a}$$

and

$$\left.\begin{aligned} e_{mn} &= j\frac{\pi\delta^2 m}{ad} - (\pi-a) + t_{mn,} \\ f_{mn} &= q_{mn} \\ v_{mn} &= j\frac{\pi\delta^2 m}{ad} - (\pi-a) - t_{mn} \\ u_{mn} &= q_{mn} \end{aligned}\right\} \text{for } m = n, \tag{12b}$$

with:

$$\begin{pmatrix} g_m = (\pi-a) - t_{11} & w_m = -q_{11} & \text{for } m = 1 \\ g_m = -t_{m1}\text{-}s_{m1} & w_m = p_{m1} - q_{m1} & \text{for } m \neq 1 \end{pmatrix}. \tag{12c}$$

The system of equations was solved numerically for a limited number of equations and coefficients. The shielding factor (*S*) was used to evaluate the shielding effectiveness of the structure (i.e., shielding factor), which represents the ratio of the magnetic fields at the middle of the cylinder B_{max} to the magnetic field at the same point for the continuous cylinder without slots B_u in such:

$$S = \frac{B_{max}}{B_u}, \tag{13a}$$

with:

$$B_u = \frac{\mu H_0}{\sqrt{1+\left(\frac{ad}{\delta^2}\right)^2}}. \tag{13b}$$

In general, the induction at the middle of the cylinder with the slots is not proportional to the excitation field and it can be represented by:

$$B\left(0,\frac{\pi}{2}\right) = -\mu H_0[(1+C_1)\hat{\boldsymbol{e}}_\rho + D_1\hat{\boldsymbol{e}}_\varphi]. \tag{14}$$

Subsequently,

$$B\left(0,\frac{\pi}{2}\right) = \mathrm{B}_\rho\hat{\boldsymbol{e}}_\rho + B_\varphi\hat{\boldsymbol{e}}_\varphi. \tag{15}$$

III. RESULTS AND DISCUSSIONS

The shielding effectiveness while utilizing a shield with a geometry of hollow-cylinder with slots is expressed through the shielding factor (S). Once *S* approaches unity, the shield performance of the hollow cylinder with slots can be approximated to the continuous cylinder. The effect of various design parameters has been investigated to analyze the magnetic flux penetration through the slot such as; the position of the slot relative

to the magnetic field lines (i.e. field orientation), slot size, and excitation frequency. Figure 2 and Fig. 3 show examples for a plot of the magnetic field flux applied to the hollow-cylindrical structure in the presence of slots at different slots' conditions.

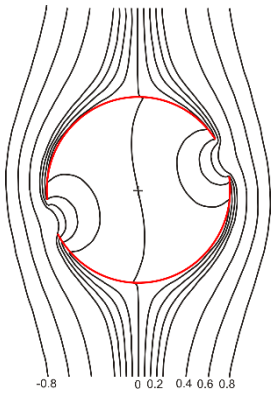

Fig. 2. Modeled magnetic field flux lines for the shielding structure with ($\frac{a.d}{\delta^2} = 5$).

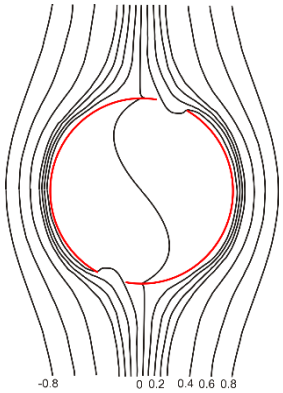

Fig. 3. Modeled magnetic field flux lines for the shielding structure with ($\frac{a.d}{\delta^2} = 10$).

As expected and away from the slot positions, the magnetic field profile exhibits a shape similar to the bulk cylinder [23]. With the presence of the slots, this profile is altered and the behavior becomes dependent on the slots' positions relative to the direction of the magnetic field flux. The effect of the geometry can be revealed by altering the shape and the behavior of the magnetic field lines by means of the presence of the induced currents.

The magnetic field lines, which are the lines of the constant vector potential in reference to $\mu a H_o$, have shown an interval of 0.8 away from the shield surface while at the interface between the conductive side and the slot have 0.2 intervals. These intervals decrease at the proximity of the slot position to a quarter of this interval value. This is due to the effect of the induced currents which provide an additional field source superimposed to the main magnetic field. This modifies the effect of the main magnetic field lines at the surface of the cylinder and causes compression of these lines. Therefore, the magnetic field penetration in the vicinity and beyond the surface of the cylinder vanishes, significantly. It can be observed from Fig. 2 that the field flux lines are coupled through the slots considerably into the interior region of the cylinder. The induced magnetic field vector can be decomposed into two components. One component is in the vertical direction and the other is in the parallel direction. The vertical field component inside the cylinder is always directed against the excitation field. Whereas the region outside the cylinder, the field adds up to the excitation field. Both slot size and its direction have a great impact on the magnetic field strength that couples through the slot. As the slot position gets closer to the horizontal line, the strength of the induced field's parallel component is greater than the vertical component. Consequently, the combined fields in the vicinity of the slot opening have a dominant parallel component compared with the vertical component, which is responsible for the fields' lines to connect through the openings. In Fig. 3, the slot position is closer to the vertical line. The vertical component of the induced field is more dominant and hence, less field couples through the slot and thereby more shielding effectiveness.

Figure 4 reveals the effect of the slot size and orientation relative to the magnetic field flux on the shielding factor of long-hollow cylinder structure with slots. The slot opening is represented by the angle α and the relative orientation of the slot to the magnetic field flux by the declination angle β. The effect of the slots' size and position relative to the magnetic field flux can be observed, as the angles α and β are modified. With the presence of the slots, the generated eddy currents got disturbed and break into two components at both ends of each slot. When increasing the slot size, the shielding factor deteriorates and the field penetration increases. This is attributed to the degradation of the counter field represented by the vertical field component generated by the shield surface at the slot position. Figure 5 shows the effect of increasing the slot size on the shielding factor of the shield at different orientations of the magnetic field lines. It is noted that for slots positioned at $\beta = 0^o$, increasing the slots' size would reduce the shielding effectiveness. This is accredited to the reduction of the induced vertical field component that is responsible to impede the excitation field.

For the angle β = 0 (i.e., when the excitation magnetic field is in parallel with the slot axis), small slot size has a negligible effect on the magnetic field shape. Under this condition, the shielding factor approaches unity and the field shape will approach the behavior of a continuous cylinder with no slots as can be observed in Fig. 4.

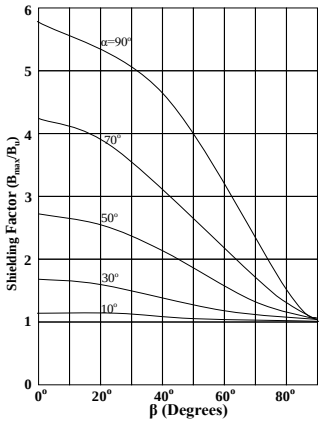

Fig. 4. The shielding factor (***S***) of the cylindrical shielding structure at different slots sizes and slots positions with ($\frac{a.d}{\delta^2} = 10$).

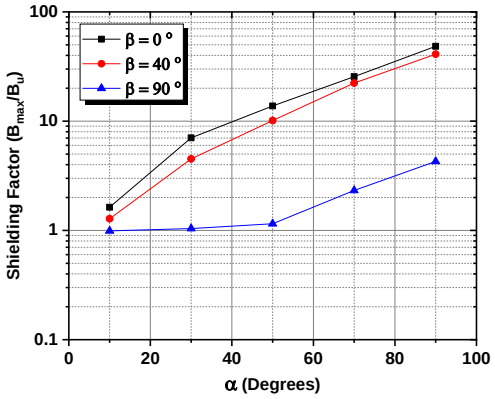

Fig. 5. The shielding factor (***S***) of a long-hollow cylinder shielding structure for different slot sizes with ($\frac{a.d}{\delta^2} = 10$).

When the slot position is modified (i.e., varying β > 0), the flux lines of the magnetic field at the center of the cylinder have shown a deflection compared with the lines without the shield. This can be due to the presence of the penetrated magnetic field through the slots. This tends to interrupt the symmetry of the structure relative to the direction of the field and thereby modifies the direction of the field lines. Similar results have been obtained by Fagnard et al. [12]. They found that the field direction at the center of the cylinder is disturbed compared with the excitation field.

Figures 2 and Fig. 3 show the shape of the magnetic field lines at the center of the cylinder while varying the position of the slots (i.e., varying β). However, a minimum variation occurs when $\beta = 90^o$, as this angle allows a direct penetration of the magnetic field lines towards the center of the cylinder. Figure 6 shows the magnetic field flux lines with $\beta = 90^o$.

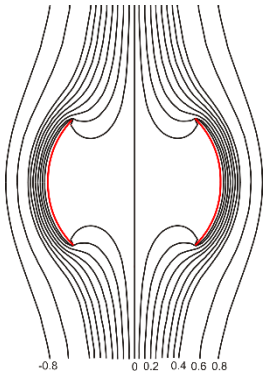

Fig. 6. Modeled magnetic field flux lines for the shielding structure at $\beta = 90^o$ with ($\frac{a.d}{\delta^2} = 10$).

The results indicate that when increasing the slot opening, the shielding factor deteriorates. However, the effect of slots' sizes is less prominent when increasing the angle β to approach the 90^o. The shielding factor for the cylinder with slots at fixed slots' sizes (i.e., fixed α) is optimal at angle $\beta = 90^o$. Figure 5 shows the behavior of the magnetic field when the pair of shielding slots is positioned in the direction of the magnetic field. At these conditions, the pair of slots is symmetrical and positioned in the direction of the excitation field. Therefore, the excitation field is directly aligned through the slots. This facilitates the direct penetration of the magnetic field through the slots.

However, the results show that regardless of the opening size of the slot, the shielding effectiveness improves in such the flux of the magnetic field at the middle of the cylinder B_{max} approaches to the magnetic field flux for the continuous cylinder B_u. Due to the highly symmetrical current distributions around the vertical line, the induced surface current densities at both conductors are equal in magnitude but opposite in direction, such that the induced magnetic field lines oppose the excitation field lines. As a result, magnetic field reduction occurs in the region inside the cylinder. Figure 6 shows the magnetic field flux lines when the slots' positions relative to the magnetic field flux is at $\beta = 90^o$ for the cylindrical shielding structure. The slot position has a significant impact on the field's vertical component strength. It has the maximum strength when $\beta = 90^o$ and it decays as β goes below 90^o. Therefore, maximum field's cancelation occurs in the inner region, while the field is strengthening in the outer region, where the field lines wrap around the conductor's exterior surface.

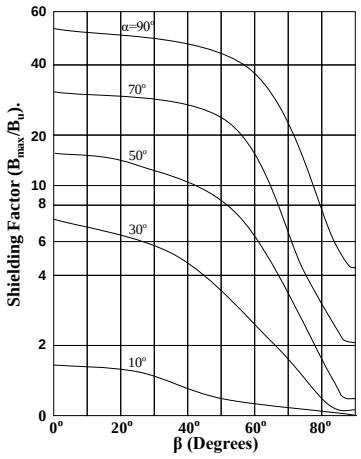

Fig. 7. The shielding factor (***S***) of the cylindrical structure at different slots sizes and positions with ($\frac{a.d}{\delta^2} = 100$).

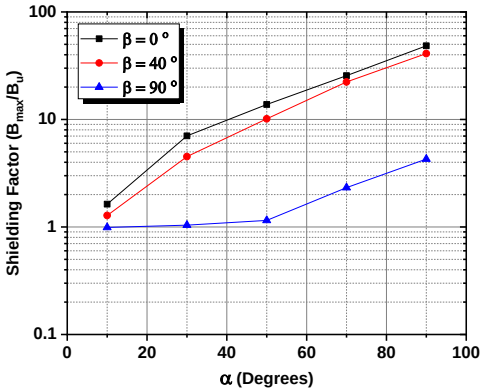

Fig. 8. The shielding factor (***S***) of a long-hollow cylinder shielding structure for different slot sizes with ($\frac{a.d}{\delta^2} = 100$).

It has been observed that when varying the excitation frequency, the behavior of the long-hollow cylindrical shielding structure with slots is the same. It is found that the shielding factor increases drastically with the excitation frequency and thereby less shielding effectiveness regardless of the slot size and positions. Figure 4 and Fig. 7 represent the effect of varying the excitation frequency (represented by the inverse proportionality relation between the excitation frequency and the skin depth while maintaining the rest of the design parameters fixed) on the shielding factor of the structure at different slots' sizes and positions. For $\alpha = 30^o$, $\beta = 40^o$ the shielding factor was 1.37 at $a.d/\delta^2 = 10$ (which indicates a low-frequency range). While at the same conditions, the shielding factor increases to about 4.51 at $a.d/\delta^2 = 100$. This indicates that at low-frequency ranges, in particular, the efficiency of the shield with slots is higher compared with the high-frequency ranges. Additionally, the effect of increasing the excitation frequency can be observed at slots' position of $\beta = 90^o$ (see Fig. 8 compared with Fig. 5).

VI. CONCLUSIONS

In this paper, modeling of the magnetic field for a long hollow cylinder with slots has been presented. The aim is to evaluate the impact of slots integration while considering the shielding effectiveness of the shielding structure and compare it with a continuous-solid conductive system. The induced eddy currents in a thin conductive system with slots have been calculated. The influence of the slot size, relative position to the excitation field, and frequency of excitation were investigated. The shielding factor was determined numerically for specific points inside the shielded space. The results show that for small slots' sizes the shielding effectiveness is comparable with the continuous cylinder structure. Additionally, positioning the slots relative to the direction of the excitation magnetic field (i.e., increasing β improves the shielding effectiveness; benefiting from the symmetry in the structure. Such a study expands on the concepts of electromagnetic shielding topology by including some considerations related to the reduction of interference utilizing the structure relative to the magnetic fields; targeting instrumentation system applications.

REFERENCES

[1] S. C. Tang, S. Y. R. Hui, and H. S. H. Chung, "Evaluation of the shielding effects on printed-circuit-board transformers using ferrite plates and copper sheets," *IEEE Trans. Power Electron.*, vol. 17, no. 6, pp. 1080-1088, 2002.

[2] F. Wen and X. Huang, "Optimal magnetic field shielding method by metallic sheets in wireless power transfer system," *Energies*, vol. 9, no. 9, pp. 733-748, 2016.

[3] Y. Kitano, H. Omori, T. Morizane, N. Kimura, and M. Nakaoka, "A new shielding method for magnetic fields of a wireless EV charger with regard to human exposure by eddy current and magnetic path," in *Proceedings - 2014 International Power Electronics and Application Conference and Exposition, IEEE PEAC 2014*, pp. 778-781,2014.

[4] L. Di Rienzo, "Modelling of magnetic current sensors for measuring high AC and DC currents," *Meas. Control*, vol. 34, no. 9, pp. 272-275, 2001.

[5] A. M. K. Dagamseh, C. M. Bruinink, R. J. Wiegerink, T. S. J. Lammerink, H. Droogendijk, and G. J. M. Krijnen, "Interfacing of differential-capacitive biomimetic hair flow-sensors for optimal sensitivity," *J. Micromechanics Microengineering*, vol. 23, no. 3, pp. 035010-035026, 2013.

[6] X. Yang, C. Xie, Y. Wang, Y. Wang, W. Yang, and G. Dong, "Optimization design of a giant magneto resistive effect based current sensor with a magnetic shielding," *IEEE Trans. Appl. Supercond.*, vol. 24,

no. 3, 2014.
[7] X. Yang, H. Liu, Y. Wang, Y. Wang, G. Dong, and Z. Zhao, "A giant magneto resistive (GMR) effect based current sensor with a toroidal magnetic core as flux concentrator and closed-loop configuration," *IEEE Trans. Appl. Supercond.*, vol. 24, no. 3, pp. 1-5, 2014.
[8] H. Kaden, *Wirbelströme und Schirmung in der Nachrichtentechnik*. Berline: Springer, 1959.
[9] A. Lopez, L. Vojtech, and M. Neruda, "Comparison among models to estimate the shielding effectiveness applied to conductive textiles," *Adv. Electr. Electron. Eng.*, vol. 11, no. 5, pp. 387-391, 2013.
[10] H. Azizi, F. Tahar Belkacem, D. Moussaoui, H. Moulai, A. Bendaoud, and M. Bensetti, "Electromagnetic interference from shielding effectiveness of a rectangular enclosure with apertures - Circuital approach, FDTD and FIT modelling," *J. Electromagn. Waves Appl.*, vol. 28, no. 4, pp. 494-514, 2014.
[11] H. H. Park, J. H. Kwon, S. Il Kwak, and S. Ahn, "Magnetic shielding analysis of a ferrite plate with a periodic metal strip," *IEEE Trans. Magn.*, vol. 51, no. 8, pp. 1-8, 2015.
[12] J.-F. Fagnard, S. Elschner, A. Hobl, J. Bock, B. Vanderheyden, and P. Vanderbemden, "Magnetic shielding properties of a superconducting hollow cylinder containing slits: Modelling and experiment," *Supercond. Sci. Technol.*, vol. 25, no. 10, p. 104006, 2012.
[13] H. M. El-Maghrabi, "Electromagnetic shielding effectiveness calculation for cascaded wire-mesh screens with glass substrate," *Applied Computational Electromagnetics Society Journal*, vol. 33, no. 6, pp. 641-647, 2018.
[14] R. Araneo, G. Lovat, S. Celozzi, and P. Burghignoli, "Shielding effectiveness of finite width shields against low-impedance magnetic near-field sources," *2018 Int. Appl. Comput. Electromagn. Soc. Symp. Denver, ACES-Denver 2018*, 2018.
[15] T. Cvetković, V. Milutinović, N. Dončov, and B. Milovanović, "Numerical investigation of monitoring antenna influence on shielding effectiveness characterization," *Applied Computational Electromagnetics Society Journal*, vol. 29, no. 11, pp. 837-846, 2014.
[16] A. M. Hussein and P. P. Biringer, "Redistribution of current in flat conductors using magnetic bars," *J. Appl. Phys.*, vol. 55, no. 4, pp. 1188-1194, 1984.
[17] I. Mayergoyz, C. Serpico, and P. McAvoy, "Analysis of eddy currents in magnetically nonlinear conductors," *J. Appl. Phys.*, vol. 109, no. 7, pp. 2011-2014, 2011.
[18] W. G. Delinger, "Magnetic field inside a hole in a conductor," *Phys. Teach.*, vol. 28, no. 4, pp. 234-235, 1990.
[19] S. Babic, Z. Andjelic, B. Krstajic, and S. Salon, "Analytical magnetostatic field calculation for a conductor with uniform current in the longitudinal direction," *J. Appl. Phys.*, vol. 67, no. 9, pp. 5827-5829, 1990.
[20] S. He and V. G. Romanov, "Explicit formulas for crack identification in conductors using boundary measurements of direct current fields," *J. Appl. Phys.*, vol. 85, no. 9, pp. 6822-6827, 1999.
[21] J. Kvitkovic, K. Burnside, M. Zhang, and S. Pamidi, "Magnetic shielding of long paraboloid structures in the inhomogeneous magnetic field," *J. Phys. Conf. Ser.*, vol. 1559, no. 1, pp. 1-9, 2020.
[22] Y. He, B. Gao, A. Sophian, and R. Yang, *Transient Electromagnetic-Thermal Nondestructive Testing: Pulsed Eddy Current and Transient Eddy Current Thermography*. Butterworth-Heinemann, 2017.
[23] W. Carr Jr, *AC Loss and Macroscopic Theory of Superconductors*. CRC Press, 2001.

Ahmad M. Dagamseh received his Ph.D. degree from the University of Twente in the Netherlands in 2011 in MEMS. His research interests include Sensors, instrumentation systems and modeling.

Qasem M. Al-Zobi received his Ph.D. degree from the Technische Universitaet Berlin/Germany in 1990. His research interests industrial electronics and external magnetic field screening.

Qasem M. Qananwah received the Ph.D. degree in Biomedical Engineering from Karlsruhe Institute of Technology, Karlsruhe, Germany. His research interest focuses in instrumentation system, design and modeling.

Hamzeh M. Jaradat received the Ph.D. degree in Electrical and Computer Engineering from the University of Massachusetts Lowell (UML), USA. His current research includes electromagnetics modeling.